Applied Radiation and Isotopes 105 (2015) 278–289

Contents lists available at ScienceDirect

Applied Radiation and Isotopes

journal homepage: www.elsevier.com/locate/apradiso

The decays of ^{109,111}Pd and ^{111}Ag following neutron capture by Pd

K.S. Krane

Department of Physics, Oregon State University, Corvallis, OR 97331, USA

HIGHLIGHTS

- High-resolution γ-ray spectrometry in radioactive decays of ^{109}Pd, ^{111g,m}Pd, and ^{111g,m}Ag.
- Order-of-magnitude improvement in precision of γ-ray energies and intensities.
- 36 γ-rays previously unobserved in radioactive decay studies reported.
- 12 unknown and 10 roughly estimated weak β intensities replaced with precise values.

ARTICLE INFO

Article history:
Received 30 April 2015
Received in revised form
26 July 2015
Accepted 14 August 2015
Available online 15 August 2015

Keywords:
^{109}Pd
^{111g,m}Pd
^{111g,m}Ag decays
γ-ray spectroscopy
^{109}Ag
^{111}Ag
^{111}Cd energy levels

ABSTRACT

Improved precisions of the energies and intensities of the γ rays emitted in the decays of ^{109}Pd and ^{111g,m}Pd have been obtained based on a high-resolution spectroscopic study of these γ emissions from radioactive samples produced by neutron capture by natural Pd. Correspondingly improved values of the energies and β feedings of the levels in the ^{109,111}Ag daughters have been deduced. More precise energies and intensities have also been determined for the γ rays emitted in the decays of the ^{111}Pd daughter activities ^{111g,m}Ag to ^{111}Cd.

1. Introduction

The decay schemes of ^{109}Pd (13 h) and ^{111g,m}Pd (23 min and 5.5 h) are known only with relatively large uncertainties. Typically the intensities of the emitted γ rays in these decays have relative uncertainties greater than 10%, even for some of the strongest transitions. Energy uncertainties are larger than 0.1 keV and often as large as 0.5 to 1.0 keV. This is somewhat surprising, in that ^{109}Pd and ^{111}Pd lie only one nucleon removed from the valley of stability, where one commonly finds spectroscopic studies achieving intensity uncertainties of 1–2% and energy uncertainties below 0.02 keV. The large uncertainties in the transition energies have resulted in similarly large uncertainties for the deduced energies of the levels in the ^{109}Ag and ^{111}Ag daughters. Particularly in the case of the ^{111m}Pd decay, there is a significant disagreement among previous investigations regarding the relative intensity of the γ rays that follow the isomeric decay and those that follow the β decay, leading to a corresponding uncertainty in the results of experiments that depend on the intensities, such as neutron capture cross sections.

Although ^{109}Pd and ^{111g,m}Pd have fairly complex decay schemes, it is nevertheless possible to perform a detailed study of the γ-ray energies and intensities in singles mode and with a source of natural isotopic abundance. High-resolution, stabilized data processing enables the fitting of unresolved multiplets, and following the intensities as a function of time enables the assignment of transitions to particular decays based on their respective half-lives.

The previously accepted spectroscopic data on the ^{109}Pd decays have been summarized in the Nuclear Data Sheets (NDS) by Blachot (2006). The γ ray energies and intensities were obtained primarily from the studies reported by Berzins et al. (1969a), Schick and Talbert (1969), and Procházka et al. (1978). Data on the ^{111}Pd and ^{111}Ag decays were summarized in the NDS by Blachot (2009) based on experiments reported by Berzins et al. (1969b), Schick and Talbert (1969), and Kracíková et al. (1977).

E-mail address: KraneK@physics.oregonstate.edu

http://dx.doi.org/10.1016/j.apradiso.2015.08.018
0969-8043/

The present work reports a new set of spectroscopic data on the γ rays emitted in the Pd decays, with intensity uncertainties typically no greater than a few per cent and energy uncertainties generally smaller than 30 eV. Based on these measurements, level energies have been deduced in the daughter Ag isotopes also with uncertainties generally smaller than 30 eV, and from the γ-ray intensity balance at each level the corresponding β feeding intensities have been obtained. Also reported are the spectroscopic data on the ^{111g,m}Ag decays (daughter activities of ^{111}Pd) to levels of ^{111}Cd.

2. Experimental details

Sources of natural Pd metal of thickness 0.025 mm were irradiated at the Oregon State University TRIGA Reactor. Because of the short halflives of the Pd activities, irradiations were done in the fast pneumatic transfer facility (with thermal and epithermal neutron fluxes respectively 1×10^{13} and 3.5×10^{11} neutrons/cm^2/s).

The γ rays were observed with high-purity Ge detectors having efficiencies of 35–40% compared with NaI at 1332 keV. The detectors were true coaxial cylinders with diameters of 52–59 mm and lengths of 60–80 mm and were connected to a computer-based, gain-stabilized DSPEC digital signal processor (http://www.ortec-online.com/). The resolution (full width at half-maximum) was typically 1.7–1.8 keV at 1332 keV. The spectroscopic data were analyzed using the peak fitting code SAMPO (Aarnio et al., 1988) to determine energies and intensities.

The spectroscopic data on the Pd decays were obtained by counting five different samples of irradiated Pd. Samples were allowed to cool for 20–30 min following irradiation in order to reduce the intensity of the 4.7 min ^{109m}Pd. Each sample was counted for about 1.5 h at a source-to-detector distance of 20–25 cm to follow the 23 min ^{111g}Pd decays for 3–4 half-lives. Then the sample was moved to 10–15 cm and counted for about 2 days to follow the 5.5 h ^{111m}Pd and 13 h ^{109}Pd. Measuring at different source-to-detector distances enhanced the ability to identify lines with significant contributions from coincidence summing.

Typical activities at the start of counting were: ^{109}Pd – 7 MBq; ^{111m}Pd – 0.01 MBq; ^{111g}Pd – 1 MBq. The Pd samples also contained small impurities, principally ^{192}Ir (60 Bq) and ^{198}Au (600 Bq). Neither of these impurity activities had a significant effect on the measurement, as most of the Pd peaks were well isolated from the Ir or Au peaks; in the few instances where the Pd peaks overlapped those of Ir or Au, the effects of the latter could be corrected for by counting their longer-lived decays after the Pd had decayed to negligible levels. The samples also contained small amounts of daughter 7.45-d ^{111g}Ag, typically about 45 kBq; after the Pd activities had decayed away over several days, this activity was counted at smaller source-to-detector distances (5–7.5 cm) over a period of about 3 weeks to record the γ-ray spectrum.

Efficiency calibrations were accomplished using sources of ^{152}Eu and ^{133}Ba. To extend the efficiency calibration above 1408 keV, ^{24}Na and ^{207}Bi were used. Additional corrections for efficiencies at high energy were determined using a source of ^{56}Co. The behavior of the efficiency curve at low energy (below 200 keV) was checked using reactor-produced sources of ^{160}Tb, ^{169}Yb, and ^{182}Ta. Efficiency calibrations were done at each source-to-detector distance and where necessary corrected for coincidence summing (significant only at the closer distances). Empirical functions were fitted to the log–log dependence of the efficiency on energy in different regions: a 4th-degree polynomial below 250 keV, a linear dependence in the range 250–450 keV, and a different linear dependence above 450 keV.

Typical contributions to the intensity uncertainties are

Efficiency calibration ($E<250$ keV)	2%.
Efficiency calibration ($E>250$ keV)	1%.
Statistics and peak fitting ($I>10\%$)	0.1–1%.
Statistics and peak fitting ($1\%<I<10\%$)	1–5%.
Statistics and peak fitting ($I<1\%$)	5–20%.
Attenuation (low energy)	$<0.1\%$.
Dead time	$<0.01\%$.

The typical statistical uncertainties listed above are representative of the shorter-lived decays; the longer-lived decays (^{109}Pd and ^{111m}Ag) permitted more counts to be accumulated and thus produced intensity uncertainties that are often smaller than those of the shorter-lived decays, especially for the less intense peaks. In the latter cases, the intensities of peaks with even very small branching ratios could be determined with uncertainties approaching the minimum of 1%.

Energy calibrations were accomplished by counting several samples simultaneously with sources of ^{56}Mn, ^{60}Co, ^{133}Ba, ^{137}Cs, ^{152}Eu, and ^{207}Bi in various combinations. Precise values of the energies of the calibration lines were taken from the recommended values of Helmer and van der Leun (2000) and Bé et al. (2006). Energies of the stronger Pd lines were determined by direct comparison with the calibration lines in data runs in which the Pd source was counted simultaneously with the calibration sources. Then in longer data runs without the calibration sources, the weaker Pd lines were calibrated against the stronger Pd lines. In this way the weaker lines could be analyzed without interference from lines from the calibration sources.

In the energy calibration runs, the calibration lines and the stronger Pd lines typically yielded statistical and fitting energy uncertainties in the range of 1–5 eV (characteristic of a data run in which peak areas exceeded 10^5 counts), which would in principle permit a determination of the energies of the stronger Pd lines to within an uncertainty of less than 10 eV. However, this would not account for any possible systematic or other contributions to the energy uncertainties. A measure of the effect of the latter can be obtained by examining the standard deviation of a distribution of values of the energies from different measurements (based on typically 5–10 independent energy determinations from different samples or from different stages in the decay period of a single sample). The final uncertainties quoted in the present work are the larger of the combined uncertainties or the standard deviation, but in no case was the combined uncertainty permitted to extend beyond a lower limit of 10 eV.

3. Results

Fig. 1 shows the γ-ray spectrum of a Pd sample taken about 30 min after the irradiation. Strong γ rays are present from the ^{109}Pd and ^{111g,m}Pd decays. Fig. 2 shows a portion of the spectrum 1.5 days later; most of the radiations are due to decays of the 13-h ^{109}Pd and 7.45-d ^{111g}Ag.

3.1. ^{109}Pd decay

The present results for the energies and intensities of the γ rays following the ^{109}Pd decay are summarized in Table 1. For comparison, Table 1 also shows the consensus results from previous studies as compiled by the NDS (Blachot, 2006) based primarily on the work of Schick and Talbert (1969). Table 1 identifies the initial and final states of the γ emissions based on the NDS level scheme.

All transitions were checked for consistency with the expected decay half-life. For this analysis, the value of the half-life has been taken to be 13.45 ± 0.01 h. The NDS recommended half-life is 13.7012 ± 0.0024 h, based on a measurement reported by Abzouzi et al. (1990). However, this value is in disagreement with

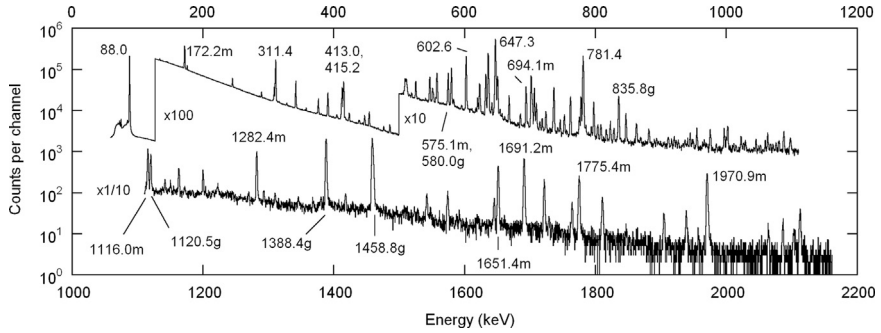

Fig. 1. Gamma-ray spectrum from irradiated Pd sample 30 min. after irradiation. Unlabeled peaks are from the decay of ^{109}Pd; peaks labeled g and m are respectively from the decays of ^{111g}Pd and ^{111m}Pd.

the 3 most precise previous measurements (as summarized in the NDS). Data from the present measurements are more consistent with the former value, which has been adopted for this analysis. The conclusions regarding the relative decay rates are unaffected by the choice of half-life, and the determination of the log *ft* values for the β decay is affected only slightly (within the margin of uncertainty in all but the most precise case). The log *ft* values were computed using the β decay *Q* values from the latest atomic mass evaluation (Wang et al., 2012).

In general, the present results (which show a considerable improvement in the precision of the energy and intensity values) are in quite good agreement with the previous results. The only minor disagreement is with the intensity of the 724.37 keV transition, for which half of our observed intensity is due to true-coincidence summing (specifically, 311.39 keV ± 413.01 keV and 309.18 keV + 415.22 keV), and an additional 25% is due to accidental summing (636.34 keV + 88.02 keV). Some additional differences between the present work and previous work are as follows:

162.37 keV The present results show a transition at 162.37 ± 0.04 keV with an intensity of 0.41 ± 0.04, which appears to decay with the 13.45 h half-life. There has been no previous report of this transition, which might fit between the levels at 869.431 and 706.967 keV (ΔE = 162.464 keV).

609.5 keV The 609.5-keV transition reported by Schick and Talbert with an intensity of 0.58 ± 0.27 was not seen in the present study (intensity < 0.03).

869.415 keV A line at 869.42 keV with an intensity of 0.22 units was observed, which would seem to agree with the corresponding line reported by Schick and Talbert with an intensity of 0.15 ± 0.08. However, the decay of this line was too rapid to agree with the expected 13.45-h half-life. At least 80% of the intensity of this line can be accounted for by coincidence summing, primarily accidental summing of the 781.39 and 88.02 keV lines (which explains the more rapid decay) but also true summing of 558.04 keV + 311.39 keV and 454.27 keV + 415.22 keV. [Other examples of accidental summing were also observed in the present spectra, including (energies in keV): 176.05 (=88.02 + 88.02), 399.42 (=311.39 + 88.02), 735.30 (=647.27 + 88.02), and 690.60 (=602.57 + 88.02). All of these lines showed a more rapid decay than would be expected for a 13.45 h half-life, which is consistent with accidental coincidence summing.] After correcting for summing, the remaining intensity of the 869-keV line is 0.06 ± 0.03. The observed energy of this line matches up nicely with the energy of the 869.431-keV level, and the small intensity is consistent with expectations for an M2 transition.

Because many of the currently accepted ^{109}Ag level energies are determined based on the energies of the γ rays emitted in the ^{109}Pd decay, the presently determined γ-ray energies can be used to obtain a more precise and self-consistent set of level energies, which are shown in Table 2. Of the 32 γ rays listed in Table 1, 26 agree with the level energy differences within 1 standard deviation and 30 agree within 2 standard deviations, which slightly exceed the numbers expected from a statistical distribution and suggest that the energy uncertainties have been neither over- nor underestimated by a significant factor. From the intensity balance at each level (including where necessary the internal conversion coefficients tabulated in the NDS), a more precise set of β feeding intensities and log *ft* values can be deduced, taking the total conversion coefficient of the 88-keV E3 transition to be 26.58 (Blachot, 2006) and assuming no direct β feeding to the ground state. These values are shown in Table 2 in comparison with the previously accepted values taken from the NDS.

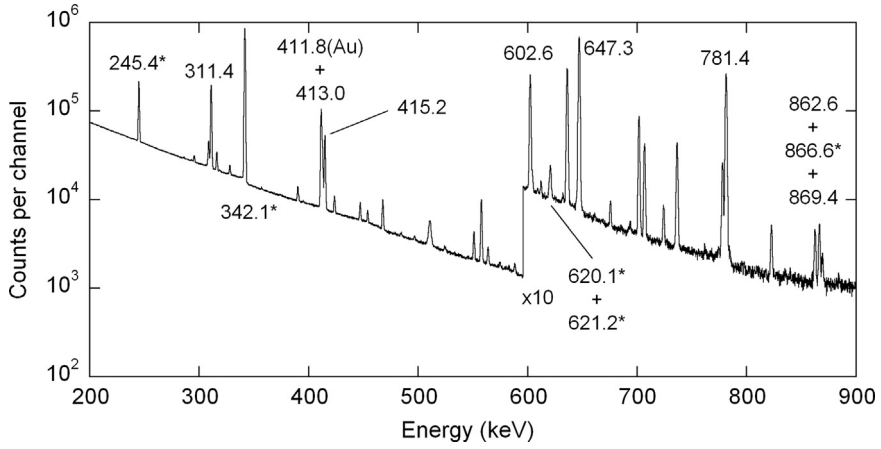

Fig. 2. Gamma-ray spectrum from irradiated Pd sample 1.5 days after irradiation. Peaks marked with asterisk are from the decay of ^{111g}Ag, others are from ^{109}Pd. The 413.0 keV peak also includes an unresolved peak at 411.8 keV from the decay of a 2.7-d ^{198}Au impurity.

Table 1
Energies and intensities of γ rays emitted in the decay of ^{109}Pd.

Previous work[a]		Present work		Levels[b]
E (keV)	*I*	*E* (keV)	*I*	
88.04(5)	14800(1400)	88.022(10)	14100(300)	*B*→*A*
103.9(4)	3.8(8)	103.827(23)	2.57(12)	*E*→*D*
134.2(2)	5.4(11)	134.107(18)	5.92(12)	*K*→*I*
145.1(2)	4.6(8)	145.039(14)	3.83(7)	*K*→*H*
		162.37(4)	0.41(4)	*K*→*G*
286.3(5)	0.58(15)	286.644(24)	0.695(48)	*F*→*E*
309.1(5)	20(6)	309.182(10)	16.3(2)	*H* →*E*
311.4(1)	131(12)	311.390(10)	130(1)	*D* →*A*
390.6(2)	3.8(8)	390.515(18)	3.51(14)	*F* →*D*
395.6(3)	0.7(3)	395.590(28)	0.282(24)	*G* → *D*
413.0(4)	27(4)	413.010(10)	27.6(3)	*H* → *D*
415.2(3)	44(4)	415.222(10)	43.9(5)	*E* → *A*
423.9(2)	3.9(8)	423.942(12)	3.83(6)	*I* → *D*
447.6(2)	3.4(8)	447.426(14)	3.74(6)	*J*→*E*
454.3(3)	2.2(9)	454.269(14)	1.71(6)	*K*→*E*
496.9(2)	0.31	497.010(23)	0.319(23)	*M*→*E*
551.4(4)	2.5(6)	551.258(14)	2.82(4)	*J*→*D*
558.1(2)	10.0(12)	558.040(10)	10.4(1)	*K*→*D*
602.5(1)	32.7(19)	602.568(10)	33.6(3)	*I*→*C*
609.5(5)[c]	0.58(27)		< 0.03	
636.3(1)	40.9(19)	636.342(10)	42.5(4)	*H*→*B*
647.3(1)	100	647.272(10)	100(1)	*I*→*B*
701.9(2)	12.7(12)	701.876(10)	13.3(1)	*F*→*A*
707.0(2)	6.5(8)	706.964(10)	6.33(6)	*G*→*A*
724.4(3)	0.77(19)	724.372(14)	0.24(3)	*H*→*A*
736.7(2)	6.9(8)	736.652(10)	6.77(7)	*K*→*C*
778.3(5)	6.2(19)	778.140(14)	4.29(5)	*L*→*C*
781.4(2)	46(5)	781.394(10)	46.6(5)	*K*→*B*
822.9(4)	0.77(12)	822.862(14)	0.759(8)	*L*→*B*
862.5(4)	0.54(12)	862.637(14)	0.682(8)	*J*→*A*
868.8(10)[c]	0.15(8)	869.415(25)	0.06(3)	*K*→*A*
966.2(3)	0.37(12)	966.29 (4)	0.145(7)	*N*→*C*
1010.0(3)	0.25(8)	1011.16 (5)	0.092(5)	*N*→*B*

[a] Values from NDS compilation (Blachot, 2006) unless otherwise indicated.
[b] See Table 2 for identification of energy levels.
[c] From Schick and Talbert (1969).

3.2. ^{111g}Pd decay

The present results for the γ rays emitted in the 23-min decay of ^{111g}Pd are shown in Table 3 and compared with the consensus of previous results from the NDS (Blachot, 2009), taken primarily from the work of Kracíková et al. (1977), Schick and Talbert (1969), and Berzins et al. (1969b). All transitions with intensity greater than 1.0 have been checked for consistency with the 23-min half-life, with the exception of 308.28, 391.23, and 415.39 keV, all of which suffer from interfering transitions in the decays of ^{109}Pd or ^{111m}Pd. Many of the transitions with intensity below 1.0 also show good agreement with the expected half-life, including 772.39, 833.5, 890.62, 937.15, 1014.69, 1049.97, 1067.87, 1269.85, 1310.93, 1506.3, 1547.83, and 1863.5 keV. The statistical uncertainties of weaker peaks are too large to permit any useful conclusions about their decay half-lives.

In general, the present results are in good agreement with previous results, with uncertainties in energy or intensity that are as much as an order of magnitude superior to the previous work. Notable differences with previous work include regions at 602 and 642 keV, where there are multiplets. The region at 602 keV is especially difficult to analyze, because about 95% of its intensity is due to the decay of ^{109}Pd. The ^{109}Pd and ^{111m}Pd peaks can be made to disappear by subtracting the data in successive 5- or 10-min spectra, enabling the ^{111g}Pd peaks to more clearly stand out. This subtraction technique was also used to isolate the intensity of the 415.39 keV peak.

As in the case of the ^{109}Pd decay, the present results for the γ-ray energies emitted by ^{111g}Pd can be used to determine a self-consistent set of energies for states in ^{111}Ag. This set of values, along with the corresponding β intensities deduced from the intensity balance at each level (assuming no direct ground-state β feeding and an internal conversion coefficient of 182 for the 60-keV transition), is shown in Table 4 and compared with the previously accepted values from the NDS. Of the 78 transitions listed with placements in Table 4, 56 (=69%) agree with the assigned level energy differences within 1 standard deviation, 74 (=92%) agree within 2 standard deviations, and 76 (=97%) agree within 3 standard deviations, which matches the expected statistical distribution. The two outliers are: (1) 493.77 keV, which misses the energy difference of the assigned levels by 9 standard deviations, and (2) 1310.93 keV, which differs from the energy difference of the previously assigned levels by 26 standard deviations. Both of these assignments should be regarded as doubtful, although neither transition fits between any other pair of known levels.

Noteworthy differences from the previous decay scheme include the following:

569 keV levels Zeghib et al. (1987) studied the levels of ^{111}Ag using the (^{3}He,pnγ) reaction and have argued for placing two levels near 569 keV, with a $5/2^+$ assignment favored for both levels. The coincidence data of Berzins et al. (1969b) show that depopulating transitions at 439 and 509 keV are in coincidence with populating transitions at 142, 494, 516, 611, 642, 937, 950, and

Table 2
Energy levels of ^{109}Ag populated in the β decay of ^{109}Pd.

Level label	Previous work[a]				Present work		
	Level energy (keV)	J^π	β feeding (%)	Log *ft*	Level energy (keV)	β feeding (%)	Log *ft*
A	0.00	$1/2^-$			0.00		
B	88.0341(11)	$7/2^+$	99.90(1)	6.130(4)	88.024(9)	99.89(1)	6.126(2)
C	132.74(11)	$9/2^+$			132.764(8)		
D	311.38(8)	$3/2^-$	0.020(4)	9.44(9)	311.385(8)	0.0207(6)	9.418(18)
E	415.21(16)	$5/2^-$	0.0057(19)	9.77(15)	415.216(7)	0.00643(25)	9.713(21)
F	701.91(15)	$3/2^-$	0.0042(4)	9.11(5)	701.880(8)	0.00451(13)	9.074(14)
G	707.00(17)		0.0018(2)	9.46(5)	706.967(9)	0.00159(6)	9.508(18)
H	724.35(10)	$(3/2)^+$	0.021(2)	8.33(5)	724.383(6)	0.0213(6)	8.318(14)
I	735.29(9)	$5/2^+$	0.032(1)	8.110(16)	735.320(8)	0.0338(10)	8.076(14)
J	862.76(20)	$5/2^-$	0.0016(3)	8.83(9)	862.643(9)	0.00187(6)	8.750(16)
K	869.47(11)	$5/2^+$	0.018(1)	7.74(3)	869.431(6)	0.0195(6)	7.693(16)
L	911.0(4)	$7/2^+$	0.0017(5)	8.51(13)	910.898(11)	0.00130(4)	8.611(17)
M	912.1	$7/2^-$			912.227(24)	0.000082(6)	9.80(4)
N	1098.5(2)	(5/2,7/2)			1099.109(32)	0.000061(6)	6.41(15)

[a] From NDS compilation (Blachot, 2006).

Table 3
Energies and intensities of γ rays emitted in the decay of ^{111g}Pd.

Previous work[a]		Present work		Levels[b]
E (keV)	*I*	*E* (keV)	*I*	
59.82(8)	63(5)	59.85(2)	74(5)	*B*→*A*
70.43(8)	90(3)	70.43(2)	93(3)	*C*→*B*
87.0	1.8			*E*→*D*
101.4(7)	0.6(3)	101.6(2)	0.3(2)	*F*→*D*
141.8(5)	0.05(2)	141.5(2)	< 0.1	*O*→*J*
166(1)	1.5(10)	166.19(5)	1.0(1)	*S*→*O*
169.4(2)	4.0(17)	169.040(28)	4.4(1)	*H*→*E*
202.2(4)	1.2(3)	202.11(6)	0.87(8)	*K*→*G*
230.3(2)	2.8(3)	230.17(3)	2.64(8)	*K*→*E*
279.0(2)	1.2(4)	279.05(5)	0.88(8)	*I*→*D*
289.8(1)	12.2(9)	289.75(3)	14.6(2)	*D*→*A*
308.4(2)	1.1(1)	308.28(5)	1.12(12)	*II*→*EE*
316.8(2)	2.4(3)	316.821(20)	2.54(10)	*E*→*B*
352.2(6)	0.7(3)	352.06(5)	0.97(9)	*L*→*D*
376.68(8)	53(3)	376.695(12)	56.4(6)	*E*→*A*
391.2(1)	3.1(1)	391.234(20)	2.8(2)	*F*→*A*
404.8(2)	10.0(6)	404.748(13)	10.1(2)	*G*→*A*
414(1)	3(1)			
415.5(3)	8.8(3)	415.39(7)	7.4(6)	*H*→*C*
418(1)	0.5(3)	417.76(4)	1.83(10)	*P*→*F*
438.5(1)	5.8(6)	438.584(15)	5.43(10)	*J*→*C*
476.7(1)	6.9(6)	476.536(19)	7.26(10)	*K*→*C*
478.9(6)	2.3(13)	478.53(5)	1.75(8)	*X*→*K*
485.8(2)	3.1(6)	485.924(19)	3.34(10)	*H*→*B*
494.1(4)	1.0(5)	493.77(5)	1.11(6)	*W*→*J*[e]
509.1(6)	25(3)	509.074(23)	24.6(3)	*J*→*B*
516.4(6)	3.1(7)	516.519(29)	2.62(8)	*X*→*J*
519.3(2)	1.2(6)	519.36(6)	1.28(8)	*P*→*D*
540.7(6)	3.1(6)	540.829(28)	2.42(8)	*Y*→*H*
547.00(8)	44(3)	547.037(10)	45.6(5)	*K*→*B*
552.6(2)	1.9(3)	552.610(25)	3.57(10)	*M*→*C*
580.00(8)	100	580.040(10)	100(1)	*O*→*C*
		595.47(10)	0.62(5)	*U*→*F*
		601.85(30)	1.0(4)	*CC*→*I*
603.1(5)	2.7(13)	603.58(30)	0.4(2)	*EE*→*K*
611.3(4)	2.1(5)	611.43(3)	1.69(5)	*DD*→*J*
623.2(1)	33(2)	623.123(15)	32.9(3)	*M*→*B*
624(1)	2.0(5)	624.733(21)	4.21(8)	*CC*→*H*
635(1)	2.5(20)	634.598(26)	1.99(8)	*DD*→*H*
		641.44(9)	1.6(5)	*EE*→*J*
641.7(2)	7.0(5)	641.95(6)	2.4(5)	*L*→*A*
		641.95(6)	3.6(5)	*II*→*S*
650.4(1)	66(3)	650.492(10)	65.9(7)	*O*→*B*
657.3(6)	2.8(3)	657.351(23)	1.98(5)	*W*→*G*
685.4(2)	6.0(7)	685.495(19)	5.3(2)	*W*→*E*
		696.90(12)	0.49(5)	*U*→*D*
709.8(2)	15.0(15)	709.954(16)	15.1(2)	*Y*→*E*
742.6(4)	2.0(5)	742.85(4)	1.57(4)	*Z*→*E*
745.7(6)	1.7(7)	746.24(4)	1.48(4)	*S*→*C*
773(1)	0.5(2)	772.39(6)	0.52(4)	*W*→*D*
775.5(3)	5.0(5)	775.561(18)	5.23(7)	*DD*→*G*
793.8(6)	2.1(4)	793.861(27)	1.99(5)	*CC*→*E*
803.8(3)	4.1(7)	803.673(22)	3.61(6)	*DD*→*E*
808.5(2)	3.2(4)	808.426(24)	3.30(6)	*II*→*O*
816.5(10)	0.9(5)	816.84(5)	0.97(4)	*S*→*B*
828(1)[c]	0.5(3)		< 0.2	
833(1)	1.0(5)	833.5(1)	0.96(4)	*EE*→*E*
835.7(2)	32(2)	835.762(17)	32.0(3)	*II*→*M*
890(1)	0.5(2)	890.62(5)	0.43(3)	*DD*→*D*
921.4(6)	2.9(6)	920.64(4)	1.41(4)	*EE*→*D*
937.3(10)	0.8(4)	937.15(6)	0.74(3)	*HH*→*J*
950.0(10)	1.0(4)	949.87(7)	0.94(3)	*II*→*J*
955.5(6)	4.5(4)	955.134(24)	3.92(5)	*X*→*C*
1002.3(3)	7.3(13)	1002.280(17)	6.05(7)	*W*→*B*
1015(1)	1.0(5)	1014.69(10)	0.64(4)	*MM*→*K*
1022(1)	0.8(4)	1022.1(2)	0.41(4)	*OO*→*M*
1026.6(10)	1.0(5)	1026.68(4)	1.03(4)	*Y*→*B*
1050.5(10)[d]	0.4(3)	1049.97(10)	0.38(2)	*DD*→*C*
1053(1)	0.5(3)	1052.6(1)	0.45(3)	*MM*→*J*
1059.8(10)	1.5(5)	1059.78(10)	1.31(4)	*Z*→*B*
1067.1(5)	1.5(5)	1067.87(7)	0.81(4)	*NN*→*K*
1098(1)	0.8(4)	1097.71(6)	0.65(4)	*OO*→*K*
1120.4(2)	16.0(15)	1120.458(17)	15.6(2)	*DD*→*B*
1246(1)	0.4(2)		< 0.1	
1269.7(5)	1.0(3)	1269.85(5)	0.91(4)	*NN*→*G*
1311.2(10)	0.9(5)	1310.93(5)	0.52(2)	*LL*→*D*[e]
1348(2)	2(1)	1346.2(3)	0.18(3)	
1388.5(2)	64(5)	1388.382(16)	58.3(6)	*II*→*C*
1395(1)	0.5(3)		< 0.1	
1459.0(3)	67(5)	1458.829(18)	61.8(6)	*II*→*B*
1506(1)	0.1(1)	1506.3(3)	0.28(3)	*HH*→*A*
1542.9(4)	2.6(3)	1542.61(3)	1.99(4)	*LL*→*B*
1549(1)	0.6(3)	1547.83(20)	0.38(2)	
1574.5(5)	3.1(5)	1574.50(3)	2.33(4)	*OO*→*C*
1644.3(10)	2.3(5)	1644.87(10)	0.99(3)	*OO*→*B*
1705(1)[c]	0.1(1)	1706.5(5)	0.09(2)	
1863.2(10)	0.3(2)	1863.5(3)	0.22(1)	
1933(1)[c]	0.1(1)	1934.1(5)	0.03(2)	

[a] From NDS compilation (Blachot, 2009) unless otherwise indicated.
[b] See Table 4 for identification of levels.
[c] From Berzins et al. (1969b).
[d] From Schick and Talbert (1969).
[e] Transition placement is doubtful.

1053 keV. Based on the present more precise energy determinations, these coincidence data are consistent with a level at 568.910 keV. Another possible depopulating transition near 279 keV was previously found not to be in coincidence with any of the populating transitions and could be placed with a second level near 569 keV. The 279-keV peak in the present spectra is clearly a doublet with both components appearing to decay with the 23 min half-life. One component at 278.01 keV is assigned to the decay of ^{111m}Ag; the second component at 279.05 keV can be assigned as the transition depopulating a level at 568.80 keV. The present results thus are consistent with two close-lying levels at 569 keV.

602 keV doublet After subtracting successive spectra to eliminate the effect of the ^{109}Pd transitions, the 602 keV region reveals the presence of two weak peaks at 601.85 and 603.58 keV. The former can be placed as depopulating the 1170.518 keV level to one of the levels at 569 keV; it has tentatively been placed as populating the level at 568.80 keV based on the failure of the previous coincidence studies to show this transition in coincidence with 509 or 439 keV. The 603.58 keV transition may connect the 1210.36 and 606.878 keV levels (ΔE = 603.48 keV). A transition of that energy was assigned to those levels by Zeghib et al.; their data would correspond to a decay intensity of 0.5 ± 0.1, in good agreement with our results.

642 keV multiplet The fit to the peak at 642 keV clearly shows it to be a doublet, with components of 641.44 keV and 641.95 keV. The former can be placed between the levels at 1210.36 and 568.910 keV (ΔE=641.45 keV). The present intensity ratio of the 641.44 and 920.64 keV γ rays from the 1210.36 keV level is 1.6/1.4=1.1, in good agreement with the (^{3}He,pnγ) results (31/24=1.3). The 641.95 keV component can be placed as depopulating the 641.88-keV level. Zeghib et al. show the intensity ratio of the 642 and 352 keV γ rays from the 641.88-keV level as 230/82=2.8, while the present ratio is 6.0/0.85=7.1 if all of the intensity of the 641.95 keV component is assigned to the 641.88-keV level. This disagreement suggests that the 641.95-keV γ ray may have a dual placement in the decay scheme, with 2.4 units assigned to the decay from the 641.88-keV level and the remaining 3.6 units assigned elsewhere. The closest fit among the present levels is 1518.714 to 876.59 keV (ΔE=642.12 keV), which is tentatively proposed as its placement in Table 3. The two proposed components of the observed 641.95-keV peak (641.88 and

Table 4
Energy levels of ^{111}Ag populated in the β decay of ^{111g}Pd.

Level label	Previous work[a]				Present work		
	Level energy (keV)	J^π	β feeding (%)	Log *ft*	Level energy (keV)	β feeding (%)	Log *ft*
A	0.00	$1/2^-$			0.00		
B	59.82(4)	$7/2^+$	95.3(4)	5.85(5)	59.86(2)	96.0(3)	5.880(3)
C	130.28(5)	$9/2^+$			130.29(3)	<0.1	>8.8
D	289.71(5)	$3/2^-$			289.75(3)	0.049(5)	8.97(5)
E	376.71(5)	$3/2^+$	0.18	8.3	376.693(11)	0.177(12)	8.34(3)
F	391.28(5)	$5/2^-$	≈ 0.027	≈ 9.1	391.236(20)	0.0055(15)	9.83(12)
G	404.86(9)	$1/2^+$			404.749(13)	<0.001	>10.6
H	545.72(6)	$7/2^+$	≈ 0.08	≈ 8.5	545.760(18)	0.055(5)	8.68(4)
I	568.67(19)	$5/2^+$	0.05	8.2	568.80(6)	<0.001	>10.4
J	568.8(2)	$5/2^+$	0.10	8.2	568.910(21)	0.160(10)	8.19(3)
K	606.87(6)	$5/2^+$	0.39	7.7	606.878(14)	0.364(22)	7.79(3)
L	641.93(7)	$3/2^-$			641.88(4)	0.025(5)	8.92(9)
M	683.05(7)	$9/2^+$			682.965(19)	0.030(4)	8.80(6)
O	710.29(7)	$(5/2^+,7/2^+)$	1.36(14)	7.1(1)	710.348(16)	1.18(7)	7.17(3)
P	809.17(9)	$5/2^-$	≈ 0.018	≈ 8.8	809.03(4)	0.023(3)	8.77(6)
S	876.63(8)	$9/2^+$	≈ 0.022	≈ 8.7	876.59(3)	<0.003	>9.6
U	986.82(8)	$5/2^-$			986.69(8)	0.0081(7)	9.00(4)
W	1062.27(15)	$3/2^+$	0.16	7.6	1062.151(13)	0.101(6)	7.80(3)
X	1085.48(8)	$(7/2^+)$	≈ 0.07	≈ 7.9	1085.425(23)	0.060(4)	7.99(3)
Y	1086.64(10)	$(3/2^+,5/2^+)$	0.16	7.5	1086.619(16)	0.139(9)	7.62(3)
Z	1119.68(10)	$(3/2^+)$	0.10	7.7	1119.56(4)	0.023(2)	8.36(4)
CC	1170.2(4)	$(3/2^+,5/2^+)$	≈ 0.034	≈ 8.1	1170.518(22)	0.052(5)	7.93(5)
DD	1180.16(10)	$5/2^+$	0.17	7.4	1180.334(12)	0.222(14)	7.28(3)
EE	1210.38(9)	$3/2^+$	0.10	7.5	1210.36(4)	0.034(4)	8.05(6)
HH	1506.0(5)				1506.08(6)	0.0074(6)	8.17(4)
II	1518.68(9)	$5/2^+,7/2^+$	1.4(2)	5.8(1)	1518.714(13)	1.18(7)	5.94(3)
LL	1602.5(4)	$5/2^+$	≈ 0.029	≈ 7.3	1602.48(3)	0.0145(9)	7.66(3)
MM	1621.3(4)	$3/2^+$	≈ 0.013	≈ 7.6	1621.54(7)	0.0079(6)	7.88(4)
NN	1674.5(4)	$(3/2)^-$	≈ 0.021	≈ 7.2	1674.66(4)	0.0125(9)	7.54(4)
OO	1705.11(11)	$(5/2^+,7/2^+)$	≈ 0.06	≈ 6.7	1704.75(3)	0.032(2)	7.05(3)

[a] From NDS compilation (Blachot, 2009).

642.12 keV) cannot be resolved in the present spectra but their combination would result in a peak energy very close to the observed value.

808 keV A transition of energy near 808 keV was previously assigned to two locations in the decay scheme in the NDS, one of which was a ground-state transition from the 809-keV level. The present data show no doublet structure in this line, and the measured energy (808.426 keV) makes it unlikely that this transition can be assigned to depopulate the level at 809.03 keV. Instead, all of the intensity is assigned as connecting the levels at 1518.714 and 710.348 keV ($\Delta E = 808.366$ keV).

1518.714 keV level The data of Zeghib et al. show the 1458.829 and 1388.382 keV peaks, both of which are assigned as depopulating the 1518.714-keV level, with an intensity ratio of 0.47 ± 0.03, whereas the present decay data show that ratio to be 1.053 ± 0.014. Previous decay data agree with the latter ratio with an uncertainty of the order of 10%. This discrepancy between the reaction and decay data would seem to suggest that there is an alternate placement for about half the intensity of the 1388.382 keV line in the (^{3}He,pnγ) experiment or for about half of the 1458.829 keV intensity in the decay studies.

3.2.1. New or unplaced transitions

Table 3 lists several transitions previously reported in decay studies but not included among the γ rays in the NDS compilation (828, 1049.97, 1706.5, 1934.1 keV). All except 828 keV were observed in the present study, but only 1049.97 keV was strong enough to be able to verify its decay with the 23-min halflife. Two other transitions observed in the present work to decay with the 23-min halflife (and previously unreported in decay studies but reported in the reaction study) are

595.47 ± 0.10 keV ($I = 0.62 \pm 0.05$, $U \rightarrow F$)
696.90 ± 0.12 keV ($I = 0.49 \pm 0.05$, $U \rightarrow D$)

The intensity ratio of these transitions deduced from the reaction studies, 1.2 ± 0.1, agrees very well with that of the present study, 1.26 ± 0.16, from which it can be concluded that the reaction and decay studies are observing the same transitions. These two transitions are also observed in the decay of the metastable state, but the half-life observed here shows that these components originate from the ground-state decay.

Other previously unreported transitions observed in the present study to decay consistent with the 23-min half-life and whose energy agrees (within two standard deviations) with energy differences of the known levels are

573.38 ± 0.08 keV ($I = 1.6 \pm 0.2$, $DD \rightarrow K$)
681.84 ± 0.08 keV ($I = 0.47 \pm 0.05$, $Y \rightarrow G$)
714.97 ± 0.08 keV ($I = 0.23 \pm 0.03$, $Z \rightarrow G$)
805.49 ± 0.08 keV ($I = 0.34 \pm 0.04$, $EE \rightarrow G$)
911.87 ± 0.09 keV ($I = 0.60 \pm 0.04$, $II \rightarrow K$)
1150.54 ± 0.08 keV ($I = 1.1 \pm 0.1$, $EE \rightarrow B$)

In the absence of coincidence data, these suggested assignments should be regarded as very tentative. Other transitions showing the 23-min half-life but not able to be accommodated among the known levels are

756.15 ± 0.08 keV ($I = 0.56 \pm 0.05$)
1080.18 ± 0.10 keV ($I = 0.64 \pm 0.09$)
1147.33 ± 0.10 keV ($I = 0.26 \pm 0.08$)
1171.86 ± 0.10 keV ($I = 0.58 \pm 0.05$)

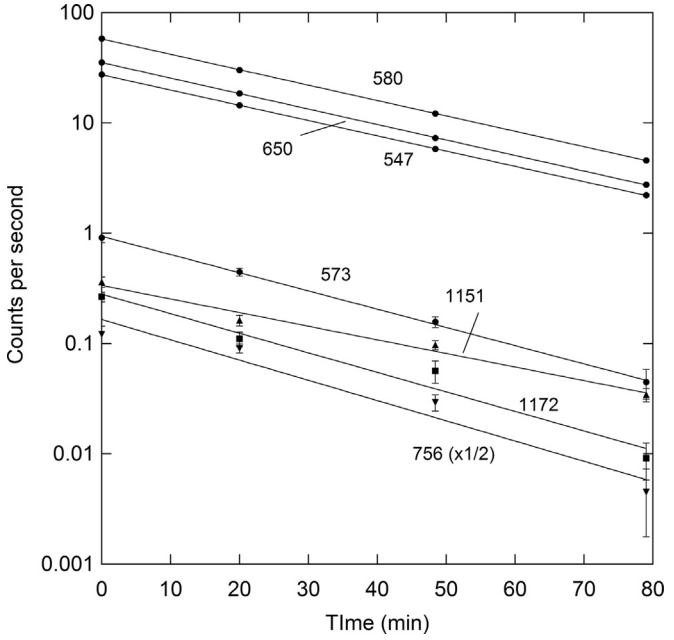

Fig. 3. Decay with time of newly proposed lines in the ^{111g}Pd decay compared with the time dependence of the 3 strongest lines in the decay. A small impurity in the 1151-keV line may be causing a 10% larger effective half-life for that line.

Fig. 3 shows the decays with time of some of the newly identified lines, compared with the time dependence of the 3 strongest lines in the ^{111g}Pd decay. Such decay curves permit the ready identification of even very weak lines that decay with the 23-min half-life.

3.3. ^{111m}Pd decay

Table 5 shows the deduced energy and intensity values for the γ rays following the decay of 5.5-h ^{111m}Pd compared with the NDS compilation. With the exception of the 172.17-keV isomeric transition, all listed γ rays represent transitions in ^{111}Ag that follow the β decay of ^{111m}Pd; γ rays resulting from decays of ^{111m}Pd through the isomeric transition and the ensuing β decay of ^{111g}Pd have been excluded from Table 5. The data in Table 5 were obtained from the irradiated Pd samples beginning about 2–3 h following the irradiation and lasting for about 10–15 h thereafter. At the beginning of the data accumulation there was a negligible amount of ^{111g}Pd remaining from the original irradiation. The presence of ^{109}Pd had only a small effect on the analysis. All peaks with intensity greater than 1.0 (except for those in the complex multiplets at 308–316 and 410–415 keV) were checked for agreement of their decay with the 5.5-h half-life.

The peaks at 307.4 and 316.6 keV suffered considerable interference (respectively about 50% and 75% of their intensities) from unresolved γ rays from the decay of ^{192}Ir, which was present as an impurity in the samples. These were nevertheless easily correctable by counting the source after several weeks, when the Pd had disappeared and only the Ir remained. Nevertheless, the result of this subtraction was rather large relative uncertainties in the energies and intensities of these two transitions. The 410–415 keV region shows strong interference from the 413.010- and 415.222-keV γ rays emitted by ^{109}Pd; approximately 95% of the 413- and 415-keV peak intensities are due to the ^{109}Pd decays. By subtracting successive 3-h spectra, it was possible to strip the contributions from ^{109}Pd from the data. The remaining 413- and 415-keV lines showed the expected 5.5-h decay.

The present results are generally in good agreement with previous work (as summarized in the NDS), with improvements in

Table 5
Energies and intensities of γ rays emitted in the decay of ^{111m}Pd.

Previous work[a]		Present work		Levels[b]
E (keV)	*I*	*E* (keV)	*I*	
59.77(4)	4.8(3)	59.7(2)	5(3)	*B*→*A*
70.44(7)	378(27)	70.44(2)	422(32)	*C*→*B*
87.0	1.45			*E*→*D*
101.8(1)	14(2)	101.39(15)	15.2(12)	*F*→*D*
118.7(6)	5(3)	119.2(1)	7(2)	*Q*→*N*
166(1)	5(3)	166.47(10)	4.3(4) 10(2)	*S*→*O* *VV*→*SS*
169.1(5)	22(7)	168.97(3)	37.9(8)	*H*→*E*
172.18(8)	1750(150)	172.170(10)	2082(42)	
178(1)[c]	1.3(8)		< 0.3	
259.5(5)[d]	4.1(14)		< 0.7	
263(1)[c]	1.0(5)		< 0.5	
272.0(2)	8.3(8)	272.08(5)	8.5(3)	*SS*→*KK*
289.8(1)	52(5)	289.727(15)	53.3(15)	*D*→*A*
308.1(4)	7(3)	307.4(3)	4.4(7)	*AA*→*R*
316.9(7)	1.85	316.6(3)	2.5(10)	*E*→*B*
357.9(1)	21(2)	358.048(18)	23.9(8)	*SS*→*GG*
376.7(1)	44(6)	376.698(14)	40.2(6)	*E*→*A*
381.0(5)[d]	2(1)	380.85(20)	2.7(5)	*SS* →*FF*[e]
391.3(1)	270(22)	391.258(10)	272(3)	*F*→*A*
413.5(3)	89(21)	413.65(20)	83(5)	*T*→*H*
415.5(3)	81(18)	415.39(7)	90(7)	*H*→*C*
418(1)	2.7(13)	417.72(4)	14.4(3)	*P*→*F*
439.3(2)	12.1(20)	439.422(23)	12.6(4)	*GG*→*V*
444.2(2)	6.3(7)	444.30(6)	5.0(2)	
454.5(2)	13(5) 56(9)	454.43(4)	66(2)	*BB*→*N* *R*→*F*
465.7(10)[d]	5(2)		< 0.5	
467.2(10)[d]			< 1	
477(1)	< 2	476.57(10)	1(1)	*GG*→*U*
485.9(1)	26(4)	485.895(15)	26.6(3)	*H*→*B*
519.3(2)	7.5(8)	519.22(3)	8.7(5)	*P*→*D*
525.6(1)	65(7)	525.613(14)	66.4(6)	*KK*→*V*
552.2(2)	14(3)	552.50(4)	9.4(2)	*PP*→*AA*
552.6(2)	1.2(4)		2.3(3)	*M*→*C*
556.1(1)	14(2)	555.94(4)	9.5(3)	*R*→*D*
575.0(1)	159(15)	575.064(10)	163(2)	*N*→*C*
583.4(4)	13(3)	583.407(27)	15.1(5)	*JJ*→*T*
595.4(5)	6.3(6)	595.50(5)	6.7(2)	*U*→*F*
617.5(3)	3.5(20)	617.62(4)	5.4(2)	*GG*→*R*
623.2(3)	20(6)	623.116(14)	20.6(4)	*M*→*B*
632.8(2)	178(15)	632.583(10)	171(2)	*V*→*F*
645.6(5)	5(3)	644.82(7)	4.0(9)	
654.7(2)	7.5(8)	654.286(18)	11.0(8)	*GG*→*P*
668.5(2)	49(5)	668.159(14)	47.5(5)	*SS*→*AA*
694.2(1)	100	694.088(10)	100(1)	*Q*→*C*
697(1)	7(4)	696.963(28)	3.8(1)	*U*→*D*
703.8(2)	33(4)	703.673(14)	39.5(4)	*KK*→*R*
716(1)	2(1)	715.36(4)	3.9(3)	*R*→*C*
718.9(2)	9(3)	718.852(23)	9.0(3)	*PP*→*U*
724.8(2)	14.0(13)	724.445(16)	14.3(4)	*QQ*→*V*
745.6(5)	6.3(11)	746.262(25)	6.3(3)	*S*→*C*
753.0(4)	6.0(20)	752.529(26)	8.9(4)	*TT*→*AA*
762.2(1)	63(5)	762.002(10)	58.0(6)	*AA*→*F*
797.8(1)	51(3)	797.619(14)	48.1(5)	*SS*→*V*
808.5(2)	3.4(5)	808.59(4)	1.4(3)	
817(1)	5(3)	816.68(4)	4.0(2)	*S*→*B*
828.3(5)	5.9(20) 2.8(12)	828.17(5) 829.14(12)	4.6(4) 2.6(6)	*VV*→*BB* *T*→*C*
844.7(10)[d]	1.1(7)		< 0.3	
862.8(5)	7.5(20)	863.71(20)	4.1(8)	*AA*→*D*
882.1(3)	10.7(10)	881.908(23)	7.8(2)	*TT*→*V*
894(2)	3	893.54(4)	2.4(1)	*V*→*C*
916.2(7)	5(3)	916.18(4)	1.9(1)	*WW*→*AA*
941.5(10)[d]	2.1(14)	940.79(4)	2.4(1)	*UU*→*V*[e]
944.7(5)	6.5(20)	944.784(23)	6.5(2)	*SS*→*S*
975.2(5)	8(2)	975.708(26)	8.7(2)	*SS*→*R*
984.9(10)[d]	1.4(7)	984.99(10)	1.2(1)	
996.3(4)	13(3)	996.863(26)	10.7(2)	*SS*→*Q*
1001.2(5)	5(2)	1000.35(8)	4.5(1)	*PP*→*N*
1022.5(5)	7(4)	1022.943(22)	5.8(2)	*AA*→*C*
1029.0(15)	3(2)	1029.29(3)	3.7(1)	*BB*→*C*

Table 5 (*continued*)

Previous work[a]		Present work		Levels[b]
E (keV)	*I*	*E* (keV)	*I*	
1045.2(7)	5(2)	1045.45(3)	3.9(1)	*WW*→*V*
1063.4(7)	7.4(40)	1063.454(28)	7.0(2)	*XX*→*V*
1076(1)	2(1)	1076.15(8)	2.4(1)	*RR*→*N*
1088.0(5)	10(3)	1088.095(28)	9.9(1)	*UU*→*S*
1098.5(10)	6(3)	1098.75(3)	3.5(2)	*RR*→*M*
1115.9(2)	55(5)	1116.021(17)	53.9(6)	*SS*→*N*
1139.6(7)	3(2)	1138.58(10)	0.97(10)	*SS*→*M*[e]
1142.4(7)	6(3)	1142.17(5)	4.4(2)	*YY*→*T*
1163.3(3)	17(2)	1163.332(18)	15.0(3)	*VV*→*Q*
1200.1(3)	16(2)	1200.268(22)	14.0(3)	*TT*→*N*
1222.5(5)	4.5(30)	1222.60(9)	3.2(1)	*TT*→*M*
1258.5(10)[d]	1.3(7)		< 0.3	
1270(1)	< 2		< 0.3	
1282.5(2)	52(5)	1282.421(17)	51.9(5)	*VV*→*N*
1309(1)	< 3	1310.14(4)	1.8(3)	*FF*→*C*[e]
1351.2(20)[d]	1.2(7)		< 0.3	
1381(1)	2(1)	1380.81(5)	1.8(3)	*FF*→*B*[e]
1418(1)	3(1)	1418.28(3)	3.3(2)	*YY*→*M*
1428.3(15)[d]	1.4(7)		< 0.3	
1651.3(2)	36(4)	1651.408(19)	34.4(3)	*RR*→*C*
1691.1(2)	64(5)	1691.190(18)	58.0(8)	*SS*→*C*
1721.9(2)	17(2)	1721.92(3)	13.8(2)	*RR*→*B*
1762.1(10)[d]	1.0(5)	1761.61(21)	0.69(14)	*SS*→*B*
1775.2(5)	23(3)	1775.35(3)	20.2(3)	*TT*→*C*
1905(1)	4(3)	1904.90(8)	2.9(1)	*UU*→*B*
1939(1)	5(3)	1939.19(8)	2.8(1)	*WW*→*C*
1970.8(3)	31(3)	1970.901(23)	28.2(3)	*YY*→*C*
2064.1(10)	1.4(8)	2064.23(20)	0.9(2)	
2086(1)	< 2	2087.11(20)	1.3(2)	

[a] From NDS compilation (Blachot, 2009) unless otherwise indicated.
[b] See Table 6 for identification of levels.
[c] From Berzins et al. (1969b).
[d] From Schick and Talbert (1969).
[e] Transition placement is doubtful.

the precision of the energy and intensity by as much as an order of magnitude. The present set of more precise γ-ray energies and intensities leads to the set of level energies and β feedings shown in Table 6. Of the 83 transitions listed in Table 5 with suggested placements, 52 (=63%) agree with the energy difference of the placements within 1 standard deviation, 71 (=86%) within 2 standard deviations, and 78 (=94%) within 3 standard deviations. Of the five outliers, three are members of the 454.43- and 552.50-keV unresolved doublets in which the energies of the individual peaks cannot be determined, and the remaining two are the 358.05-keV (3.5 standard deviations) and 996.86-keV (3.5 standard deviations) transitions. These latter two cases are not sufficient outliers to suggest incorrect placements.

Several transitions listed in Table 5 have been reported previously for the ^{111m}Pd decay but not assigned to specific levels. More stringent upper limits can be set on several weak γ rays reported previously. Several other transitions are identified in Table 5 that were previously reported and verified in the present study; some of these can be tentatively assigned to connect specific levels based on the good match between the transition energy and the energy difference of the levels. Other noteworthy features of the decay are the following:

166.47 keV The intensity of the 166-keV transition has been given previously as 2.5 ± 2.5 by Berzins et al. and 5 ± 3 by Kracíková et al. However, in both of these previous studies the weak 166-keV peak was unresolvable from the more intense neighboring 169- and 172-keV peaks. In the present work the 166- and 169-keV peaks are clearly resolvable, as illustrated in Fig. 4. With the 166.47-keV peak resolved, its intensity is deduced to be much larger than deduced in previous works, namely 14 ± 2. The peak has been variously placed (based on coincidence studies) as depopulating the levels at 876.556 keV (Δ*E*=166.208 keV) or 1987.764 keV (Δ*E*=166.354 keV). As this peak also appears in the decay of 23-min ^{111g}Pd, in which only the 876.556 keV level is populated, the component of the combined peak in the ^{111m}Pd decay associated with the 876.556 keV level can be determined from a comparison with the intensities of the other γ rays from that level, which in turn permits the (larger) component of its intensity associated with the decay of the 1987.764 keV level to be determined. The resulting intensities of the components of the 166-keV transition are given in Table 5.

519.22 keV The intensity of the transition at 519.22 keV was previously in part (25%) assigned to a level at 809 keV; the remaining intensity was unassigned. This division was based on the ratio between the intensities of the 519- and 418-keV γ rays measured in the (^{3}He,pnγ) work and the previously accepted intensity of the 418-keV transition. In previous γ-ray spectroscopic studies, the 418-keV γ ray was not clearly resolved from the multiplet at 413–415 keV. Because the 417.72-keV transition is clearly resolved in the present work, its intensity could be directly determined and was revealed to be considerably larger than the previous value. As a result, it can be concluded that all of the intensity of the 519.22-keV transition can be placed as depopulating the 808.960-keV level.

580 keV. The on-line NDS compilation (Blachot, 2009) currently shows a 580-keV transition emitted in the decay of the 5.5-h isomeric state, with an intensity of 100 in the present units. Although a strong 580-keV transition is emitted in the ground-state decay (see Table 3), this transition has not been reported in any of the previous studies of the beta decay of the isomer, and this transition is not shown in the print versions of the *Table of Radioactive Isotopes* (Browne and Firestone, 1986) or the *Table of Isotopes* (Firestone, 1999). As this transition is likewise not observed in the present study of the ^{111m}Pd decay, it is not included in Table 5.

645 keV The presently observed transition of energy 644.82 keV does not fit between the states associated with the previously reported 645.6-keV transition (705.366–59.86 keV, giving Δ*E*=645.51 keV). A transition at that energy cannot be placed among any of the known levels within 3 standard deviations of the energy values.

1139 keV A transition at 1139.6 keV was previously placed between the levels at 1964.662 and 824.404 keV. The presently determined energy value of 1138.58 keV does not agree with this assignment (Δ*E*=1140.258 keV), but it fits better between the levels at 1821.410 and 682.978 keV (Δ*E*=1138.432 keV).

1440 keV level The (^{3}He,pnγ) study proposed a new level at 1440.26 keV, depopulated by transitions of 1310.08 and 735.3 keV. The present studies show transitions of 1310.14 and 735.14 keV, which could depopulate a level at 1440.55 keV, consistent with the (^{3}He,pnγ) work. However, the relative intensity for those transitions in the present work (1.8/4.7=0.38) disagrees with the (^{3}He,pnγ) results (19/7=2.7). One possible resolution of this discrepancy would be for about 80% of the 735.14-keV intensity in the decay study to be assigned to a different level. A transition of 1381 keV was previously assigned to the 2087-keV level. That assignment disagrees with the improved energy-level determinations (for which Δ*E*=1381.936 keV) , but the presently measured transition energy of 1380.81 keV could connect the 1440.55- and 59.86-keV levels (Δ*E*=1380.69 keV).

3.3.1. *Possible new transitions*

Based on the agreement with the 5.5-h half-life, several new transitions might be assigned to the ^{111m}Pd decay. Some of these can be tentatively assigned to specific levels based on the

Table 6
Energy levels of ^{111}Ag populated in the β decay of ^{111m}Pd.

Level label	Previous work[a]				Present work		
	Level energy (keV)	J^π	β feeding (%)	Log *ft*	Level energy (keV)	β feeding (%)	Log *ft*
A	0.00	$1/2^-$			0.00		
B	59.82(4)	$7/2^+$			59.86(2)[b]		
C	130.28(5)	$9/2^+$	7.4(30)	8.19(19)	130.300(28)	6.7(11)	8.27(8)
D	289.71(5)	$3/2^-$			289.727(15)		
E	376.71(5)	$3/2^+$			376.698(14)		
F	391.28(5)	$5/2^-$			391.258(14)		
H	545.72(6)	$7/2^+$	1.0(7)	8.7(4)	545.720(19)	1.35(14)	9.62(5)
M	683.05(7)	$9/2^+$			682.978(24)	0.203(9)	9.298(20)
N	705.42(9)	$11/2^{(+)}$	0.4(5)	8.9(6)	705.366(30)	0.21(5)	9.26(11)
O	710.29(7)	$(5/2^+,7/2^+)$			710.348(16)[b]		
P	809.17(9)	$5/2^-$			808.960(26)		
Q	824.46(8)	$11/2^+,13/2^+$	1.2(3)	8.33(13)	824.404(29)	1.31(4)	8.340(14)
R	845.88(8)	$7/2^-$			845.676(29)		
S	876.63(8)	$9/2^+$			876.556(29)	<0.05	
T	958.96(11)	$11/2^+$	1.6(5)	8.05(16)	959.42 (11)	1.12(10)	8.26(4)
U	986.82(8)	$5/2^-$			986.711(27)		
V	1023.98(8)	$9/2^-$	0.5(4)	8.5(4)	1023.843(14)	0.15(4)	9.05(12)
AA	1153.41(8)	$7/2^-$			1153.261(13)	<0.05	
BB	1159.78(24)		0.22(13)	8.7(3)	1159.60(4)	0.18(9)	8.80(22)
FF	1440.44(10)	$7/2^+,9/2$			1440.55(5)	0.095(15)	8.66(7)
GG	1463.62(11)	$(5/2^-,7/2^-)$			1463.265(19)	0.10(3)	8.60(13)
JJ	1542.5(4)	(13/2)	0.30(8)	7.90(15)	1542.83 (11)	0.26(1)	8.044(17)
KK	1549.60(11)	$9/2^-,11/2^-$	2.1(4)	7.04(13)	1549.428(17)	1.65(4)	7.229(11)
PP	1705.86(14)	$(9/2^-)$	0.89(15)	7.09(13)	1705.57(4)	0.44(2)	7.488(20)
QQ	1748.56(13)	$11/2^-,13/2^-$			1748.291(21)	0.26(2)	7.62(4)
RR	1781.67(15)	$(9/2^+,11/2^+)$	1.2(2)	6.77(14)	1781.735(19)	0.96(2)	6.972(10)
SS	1821.59(9)	$(9/2^-,11/2^-)$	6.4(8)	5.94(14)	1821.410(9)	4.4(1)	6.211(11)
TT	1905.87(16)	$(9/2^-,11/2^-)$	1.2(2)	6.41(16)	1905.727(16)	0.96(2)	6.637(11)
UU	1964.7(4)		0.39(12)	6.70(21)	1964.662(27)	0.26(1)	7.018(18)
VV	1987.90(18)	$(13/2^-)$	1.5(3)	6.03(19)	1987.764(24)	1.38(5)	6.214(17)
WW	2069.4(5)		0.35(12)	6.3(3)	2069.367(25)	0.146(5)	6.873(17)
XX	2087.0(4)				2087.30(3)	0.119(5)	6.883(20)
YY	2101.05(25)	(11/2)	0.8(2)	5.8(3)	2101.259(25)	0.65(2)	6.081(16)

[a] From NDS compilation (Blachot, 2009).
[b] From ^{111g}Pd decay.

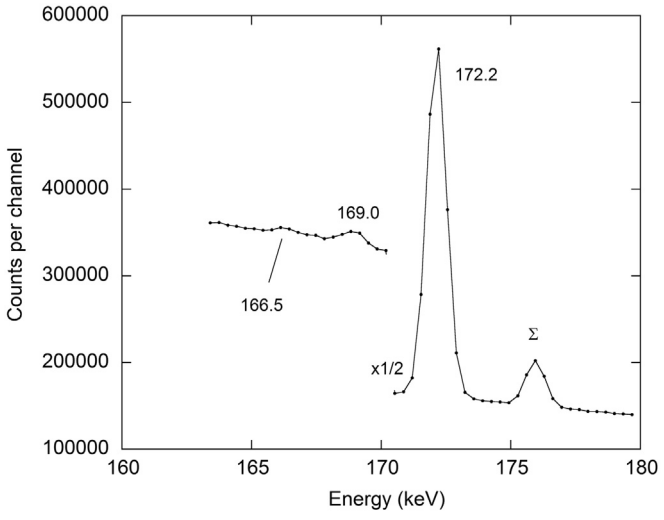

Fig. 4. Detail of spectrum of ^{111m}Pd in 170-keV region. The peak marked Σ at 176.0 keV is a sum peak due to the accidental coincidence of two 88.0-keV photons from the decay of ^{109}Pd.

agreement of the transition energy with the energy level difference (within two standard deviations)

682.02 ± 0.15 keV ($I=1.9\pm0.3$, $PP\rightarrow V$)
735.14 ± 0.10 keV ($I=4.7\pm0.6$, $FF\rightarrow N$)
785.85 ± 0.06 keV ($I=4.2\pm0.4$, $R\rightarrow B$)
859.86 ± 0.08 keV ($I=1.4\pm0.2$, $PP\rightarrow R$)
923.58 ± 0.20 keV ($I=1.3\pm0.2$, $QQ\rightarrow Q$)
926.97 ± 0.20 keV ($I=1.9\pm0.2$, $U\rightarrow B$)
948.25 ± 0.15 keV ($I=2.2\pm0.2$, $YY\rightarrow AA$)
1071.68 ± 0.10 keV ($I=2.3\pm0.2$, $RR\rightarrow O$)
1081.13 ± 0.10 keV ($I=2.6\pm0.2$, $TT\rightarrow Q$)

Other newly observed transitions which show the 5.5-h half-life but that cannot be placed between any pairs of known levels are

503.14 ± 0.10 keV ($I=1.5\pm0.5$)
605.26 ± 0.10 keV ($I=4.1\pm0.6$)
641.84 ± 0.03 keV ($I=5.6\pm0.2$)
690.41 ± 0.10 keV ($I=2.5\pm0.3$)
784.23 ± 0.10 keV ($I=7.3\pm1.0$)
869.32 ± 0.06 keV ($I=5.1\pm0.3$)
896.32 ± 0.04 keV ($I=2.2\pm0.1$)
964.14 0.12 keV ($I=1.4\pm0.1$)

Fig. 5 shows examples of how these weak peaks can be identified as part of the ^{111m}Pd decay by comparing their decay rates with those of the strong lines in the decay.

3.3.2. Intensity normalization

The absolute normalization of the intensities of the γ rays following the ^{111m}Pd β decay depends on the relative intensity of the 172.17-keV isomeric transition, which is given in the NDS as 73 ± 3% (including internal conversion). Previous decay studies gave inconsistent results for the 172.17-keV γ intensity (relative to

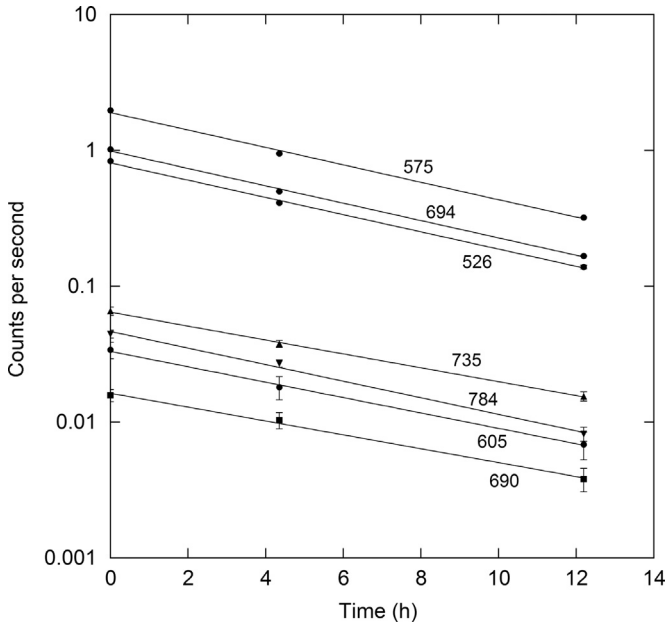

Fig. 5. Decay with time of newly proposed weak lines in the ^{111m}Pd decay compared with the time dependence of 3 strong lines in the decay.

an intensity of 100 for the 694.088-keV transition): 1525 ± 50 from Berzins et al., 2400 ± 124 from Schick and Talbert, and 1750 ± 150 from Kracikova et al., with the latter value being adopted by the NDS. The present results give a value somewhat between the extrema: 2082 ± 42. Using $\alpha = 1.17$ for the total internal conversion coefficient of the 172.17-keV transition and taking the β-decay intensities from the difference between the depopulating and populating transition intensities (γ+conversion) for the ^{111}Ag levels results in a total β intensity of $23.2 \pm 1.0\%$ and a total isomeric decay intensity of $76.8 \pm 1.0\%$, with the latter corresponding to a γ-ray intensity of $35.4 \pm 0.5\%$.

3.4. ^{111m}Ag decay

The β decay of the 64.8-s isomer at 59.86 keV in ^{111}Ag occurs too rapidly for the time behavior of its decay products to be distinguished from those of the 23-min decay of ^{111g}Pd. Thus the ^{111}Cd γ rays that follow the β decay of ^{111m}Ag will also appear to have approximately the 23-min half-life. Previous authors (Berzins et al., 1969b; Schick and Talbert, 1969; Kracíková et al., 1977) have identified several of the γ rays in ^{111}Cd that occur following the decay of ^{111g}Pd through ^{111m}Ag. The present work has been able to improve on the precision of the previous work and to observe transitions not previously reported in the ^{111g}Pd decay studies but obtained from inelastic neutron scattering (Baskova et al., 1987). Table 7 shows the results of the present experiments; for comparison, the γ intensities from the (n,n′γ) experiments have been normalized to the decay intensities using the ground-state transition from each level. The corresponding assignments of ^{111}Cd level energies and β feedings (assuming no ground-state β intensity) are given in Table 8.

3.5. ^{111g}Ag decay

Table 9 shows the energies and intensities of the γ rays in ^{111}Cd following the decay of ^{111g}Ag; results from the present work are compared with the NDS values and also with a recent measurement of the intensities by Collins et al. (2014). Also included for comparison are values for the gamma-ray intensities observed in inelastic neutron scattering work (Baskova et al., 1987). Some

Table 7
Energies and intensities of γ rays emitted in the decay of ^{111m}Ag.

Previous work				Present work		Levels[a]
^{111m}Ag decay[b]		n,n′γ[c]				
E (keV)	I	E (keV)	I	E (keV)	I	
59.77(4)	136(36)[d], 74 (10)[e]			59.85(2)	137(6)	
		96.7(2)	0.25(5)			$C \rightarrow B$
171.28(3)	24(12)	171.29(3)		171.34(6)	20.3(4)	$D \rightarrow B$
		203.29(12)	0.16(3)			$E \rightarrow D$
245.4(1)	100(7)	245.40(3)		245.373(18)	100(1)	$B \rightarrow A$
		278.04(5)	1.4(2)	278.01(9)	1.1(2)	$E \rightarrow C$
		336.16(10)	1.7(5)	336.04(5)	1.05(15)	$F \rightarrow D$
		342.12(3)		342.095(24)	8.0(7)	$C \rightarrow A$
		374.75(5)	6.9(10)	374.746(23)	6.1(2)	$E \rightarrow B$
		410.77(10)	4.7(10)	410.79(8)	3.4(3)	$F \rightarrow C$
506.9(10)	9(5)	507.6(3)	14(5)	507.41(3)	8.3(2)	$F \rightarrow B$
620.1(3)	24.1(17)	620.31(20)		620.103(19)	22.4(2)	$E \rightarrow A$
752.7(2)	8.6(10)	752.85(10)		752.828(22)	8.2(2)	$F \rightarrow A$

[a] See Table 8 for identification of levels.
[b] From NDS compilation of decay studies (Blachot, 2009) unless otherwise indicated.
[c] From Baskova et al. (1987), normalized to the decay intensities using ground-state transition from each level.
[d] From Schick and Talbert (1969).
[e] From Kracikova et al. (1977).

Table 8
Energy levels of ^{111}Cd populated in the β decay of ^{111m}Ag.

Level label	Previous work[a]				Present work		
	Level energy (keV)	J^π	β feeding (%)	Log ft	Level energy (keV)	β feeding (%)	Log ft
A	0.00	$1/2^+$			0.00		
B	245.390 (16)	$5/2^+$	0.29(13)	5.51(23)	245.377 (14)	0.248 (13)	5.579(24)
C	342.135 (16)	$3/2^+$			342.091 (22)		
D	416.72 (3)	$7/2^+$	0.12(8)	5.5(3)	416.76 (4)	0.081(4)	5.716(23)
E	620.18 (3)	$5/2^+$	0.16(6)	4.89(21)	620.111 (15)	0.124(6)	4.997(23)
F	752.81 (5)	$5/2^+$	0.14(4)	4.66(23)	752.822 (17)	0.088(5)	4.67(3)

[a] From NDS compilation (Blachot, 2009).

previous decay experiments summarized in the NDS have suggested the presence of two $3/2^+$ levels near 866 keV separated by about 1–2 keV with decay intensities to the ground state in the ratio of about 2:1, and similarly for the decay intensities to the 342.1-keV state. If two such levels existed, broadening of the γ rays at 866 and 524 keV should have been observable in the present experiments. Fig. 6 shows the full-width at half-maximum of the γ rays from 96 through 1460 keV; only at 620 keV is there a significant deviation from the smooth trend with FWHM$\propto E^{1/2}$. The known doublet at 620 keV has a 1-keV separation and a 2:1 intensity ratio of the transition intensities. A doublet of separation 1–2 keV with intensity components in the ratio of 2:1 would have produced a noticeable broadening of the peaks at 524 and 866 keV, but no such broadening is observed. If there is a second level at 866 keV, it is either separated from the main component by less than 0.25 keV or it produces decays of such low intensity that they are hidden in the tails of the stronger peaks at 524 and 866 keV (thus contributing negligibly to the FWHM). The present data therefore do not support a second level at 866 keV separated

Table 9
Energies and intensities of γ rays emitted in the decay of ^{111g}Ag.

Previous work				Present work		Levels[a]
^{111g}Ag decay			n,n′γ[b]			
E (keV)[b]	I[b]	I[c]	E(keV)	E (keV)	I	
96.75(2)	1.73(9)	1.524(14)	96.7(2)	96.718(10)	1.46(3)	$C\rightarrow B$
245.40(2)	18.5(10)	16.66(11)	245.40(3)	245.391(10)	16.4(2)	$B\rightarrow A$
278.3(4)	0.008(2)		278.04(5)	277.98(10)	0.012(4)	$E\rightarrow C$
342.13(2)	100	100	342.12(3)	342.110(10)	100(1)	$C\rightarrow A$
374.6(2)	0.047(2)	0.0360(9)	374.75(5)	374.703(28)	0.041(2)	$E\rightarrow B$
		0.00721(17)	449.81(10)	449.79(10)	0.005(3)	$I\rightarrow D$
509.4	0.02					$G\rightarrow B$
522.4(4)	0.014(2)					
524.3(4)	0.031(2)	0.0563(13)	524.33(20)	524.438(14)	0.054(1)	$I\rightarrow C$
619.3(4)	0.008(4)					
620.3(4)	0.164(12)	0.1322(14)	620.31(20)	620.100(14)	0.134(2)	$E\rightarrow A$
622.0(4)	0.09(3)	0.242(4)	621.2(4)	621.170(14)	0.242(3)	$I\rightarrow B$
754.6(4)	0.04				<0.003	$G\rightarrow A$
865.1(4)	0.023(4)					
867.0(4)	0.054(4)	0.1157(11)	866.61(10)	866.558(14)	0.110(2)	$I\rightarrow A$

[a] See Table 10 for identification of levels.
[b] From NDS compilation (Blachot, 2009).
[c] From Collins et al. (2014)

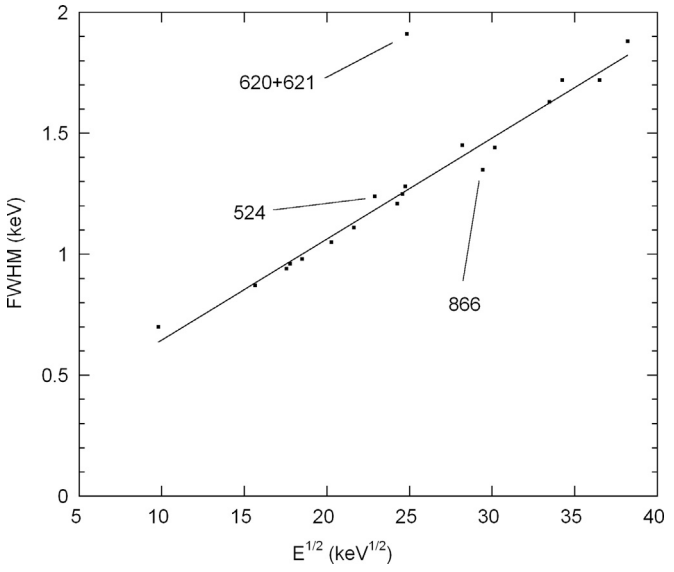

Fig. 6. Full-width at half-maximum (FWHM) of peaks in Pd spectrum showing anomalous width of 620+621 doublet in contrast to normal widths of peaks at 524 and 866 keV.

Table 10
Energy levels of ^{111}Cd populated in the β decay of ^{111g}Ag.

Level label	Previous work[a]				Present work		
	Level energy (keV)	J^π	β feeding (%)	Log ft	Level energy (keV)	β feeding (%)	Log ft
A	0.00	$1/2^+$	92(5)	7.3(2)	0.00	92.0(2)	7.322(3)
B	245.390 (16)	$5/2^+$	1.0(2)	9.2(1)	245.392 (7)	1.00(5)	9.237(14)
C	342.135 (16)	$3/2^+$	7.1(5)	7.8(1)	342.112 (7)	6.95(10)	7.813(7)
E	620.18 (3)	$5/2^+$	0.022	9.5	620.101 (13)	0.0125(4)	9.741(16)
G	754.9(4)	$3/2^+$	0.004	9.7		<0.0002	
H	864.8(3)	$3/2^+$	0.009	8.6			
I	866.60 (6)	$3/2^+$	0.013	8.4	866.559 (9)	0.0275(4)	8.193(13)

[a] From NDS compilation (Blachot, 2009).

by 1–2 keV and producing decays of approximately half the intensity of the decays from the first 866-keV level. Similarly, only a single state at 866 keV is reported in the (n,n′γ) studies (Baskova et al., 1991). The relative intensity of the 866, 621, 524, and 450 keV γ rays from the 866 keV level in the (n,n′γ) experiments is $1:1.6\pm0.4:0.55\pm0.12:0.076\pm0.024$, in excellent agreement with the corresponding ratios from the present work, $1:2.20\pm0.03:0.49\pm0.01:0.046\pm0.027$. If there were a second $3/2^+$ level at 866 keV, it might be expected that these two different types of experiments would lead to different relative populations of the two levels and thus to different relative decay intensities. The good agreement between these two results suggests the lack of strong evidence for a second level. Assuming only a single level at 866 keV, the present results lead to the ^{111}Cd level energies and β feedings presented in Table 10. The β intensities have been normalized such that the absolute intensity of the 342.11-keV γ ray is 6.68% as given by Nethaway et al. (1977) and Collins et al. (2014), with respective uncertainties of $\pm0.33\%$ and $\pm0.07\%$. The latter uncertainty has been adopted for the present analysis.

4. Discussion

In the present study, the energies and intensities of the γ rays emitted in the decays of ^{109}Pd and ^{111}Pd have been obtained with typically an order of magnitude smaller uncertainty than was characteristic of previous studies. The ^{111}Pd decays present a particular problem: the large Q value, in excess of 2 MeV, and the relatively high density of final states in the daughter ^{111}Ag, result in more than 150 γ rays populating more than 50 levels, against a background of the longer-lived decay of ^{109}Pd present in irradiated samples of natural abundance. Nevertheless, with high-resolution detectors and stabilized electronics, by following the time evolution of the γ ray intensities it is possible to unfold the complex spectra and clearly associate each line with its proper decay process, including several instances of incompletely resolved peaks from different decays. As a result, the level schemes of the ^{109}Pd and ^{111}Pd daughters have been elucidated: level energies have been deduced with an order of magnitude increased precision, and a more consistent set of β decay feeding intensities has been determined, with numerous precise β branchings at the 0.01–0.1%

level replacing unknown or roughly estimated values from the previous ^{111}Pd decay schemes.

In the cases of the (much less complex) decays of the ^{111}Ag daughters to levels in ^{111}Cd, the present work has observed several γ-ray transitions known from reaction studies such as Coulomb excitation, radiative neutron capture, and inelastic neutron scattering but not previously observed in decay studies. The addition of the corresponding results from the present decay study offers a satisfying complement to the γ-ray spectroscopy from the reaction experiments.

Acknowledgments

The support of the Oregon State University Radiation Center and the assistance of its staff in enabling these experiments to be carried out are acknowledged with appreciation.

References

Aarnio, P.A., Routti, J.T., Sandberg, J.V., 1988. MicroSAMPO – personal computer based advanced gamma spectrum analysis system. J. Radioanal. Nucl. Chem. 124, 457–465.

Abzouzi, A., Antony, M.S., Ndocko Ndongué, V.B., Oster, D., 1990. Redetermination of several half-lives. J. Radioanal. Nucl. Chem. Lett. 145, 361–368.

Baskova, K.A., Vovk, A.B., Gerus, T.M., Gorov, L.I., Demidov, A.M., Kurkin, V.A., 1987. Study of γ-rays from ^{111}Cd and ^{113}Cd from the reactions (n,n'γ) and (n,γ). Report IAE-4544/2. See also Nemeth, Zs., 1991. Low-spin levels of ^{111,113}Cd. Karlsruhe Kernforschungszentrum Report KFK 4888. Data from these unpublished works are summarized in Blachot 2009.

Bé, M.-M., Chisté, V., Dulieu, C., Browne, E., Chechev, V., Kuzmenko, N., Helmer, R., Kondev, F., MacMahon, D., Lee, K.B., 2006. Table of Radionuclides (Vol. 3 – A = 3 to 244). Monographie BIPM-5. Bureau International des Poids et Mesures, Sévres.

Berzins, G., Bunker, M.E., Starner, J.W., 1969a. Ge(Li)–Ge(Li) coincidence studies of the decay of ^{109}Pd. Nucl. Phys. A 114, 512–528.

Berzins, G., Bunker, M.E., Starner, J.W., 1969b. The decay of ^{111}Pd and ^{111m}Pd. Nucl. Phys. A 126, 273–299.

Blachot, J., 2006. Nuclear data sheets for A=109. Nucl. Data Sheets 107, 355–506 (Available online through the National Nuclear Data Center, http://www.nndc.bnl.gov/ensdf/).

Blachot, J., 2009. Nuclear data sheets for A=111. Nucl. Data Sheets 110, 1239–1407 (Available online through the National Nuclear Data Center, http://www.nndc.bnl.gov/ensdf/).

Browne, E., Firestone, R.B., 1986. Table of Radioactive Isotopes. John Wiley & Sons, New York.

Collins, S., Keightley, J., Gilligan, C., Gasparro, J., Pearce, A., 2014. Determination of the gamma emission intensities of ^{111}Ag. Appl. Radiat. Isot. 87, 107–111.

Firestone, R.B., 1999. Table of Isotopes. John Wiley & Sons, New York.

Helmer, R.G., van der Leun, C., 2000. Recommended standards for γ-ray energy calibration (1999). Nucl. Instr. Methods Phys. Res. A 450, 35–70.

Kracíková, T., Procházka, I., Hons, Z., Fišer, M., Kuklík, A., 1977. The decay of ^{111g}Pd and ^{111m}Pd. Czech. J. Phys. B 27, 1099–1110.

Nethaway, D.R., Prindle, A.L., Myers, W.A., Fuqua, W.C., Kantelo, M.V., 1977. Fission of ^{240}Pu with 14.8-MeV neutrons. Phys. Rev. C 16, 1907–1918.

Procházka, I., Kracíková, T.I., Jahelková, V., Hons, Z., Fišer, M., Jursík, J., 1978. The decay of ^{109g}Pd. Czech. J. Phys. B 28, 134–140.

Schick Jr., W.C., Talbert Jr., W.L., 1969. Gamma-ray decay schemes of ^{109g}Pd, ^{111g}Pd and ^{111m}Pd. Nucl. Phys. A 128, 353–387.

Wang, M., Audi, G., Wapstra, A.H., Kondev, F.G., MacCormick, M., Xu, X., Pfeiffer, B., 2012. The AME2012 atomic mass evaluation: (II) tables, graphs, and references. Chin. Phys. C 36, 1603–2014.

Zeghib, S., Rickey, F.A., Samudra, G.S., Simms, P.C., Wang, N., 1987. ^{111}Ag utilizing the (^{3}He, pnγ) reaction: a rotational nucleus with intermediate deformation. Phys. Rev. C 36, 939–953.